

Dielectric theorem within the Hartree-Fock-Bogoliubov framework

Luigi Capelli,^{1,*} Gianluca Colò,^{1,†} and Jun Li^{1,2,‡}

¹*Dipartimento di Fisica and INFN, Sez. di Milano, via Celoria 16, 20133 Milano, Italy*

²*School of Physics, and State Key Laboratory of Nuclear Physics and Technology, Peking University, 100871 Beijing, People's Republic of China*

(Received 17 December 2008; published 29 May 2009)

Excitation spectra usually reveal important features of the many-body systems. The vibrational excitations can be studied through the well-known linear response theory. This theory is realized, in the nuclear case, by means of the random-phase approximation (RPA); the generalization in the case in which one deals with open shells, and the pairing force is active, is the quasiparticle RPA (QRPA). It is useful to have at one's disposal theorems that provide information on, e.g., the sum rules and mean excitation energies associated with given external operators acting on the system. This article focuses on such theorems in the case of self-consistent QRPA based on Hartree-Fock-Bogoliubov (HFB). In particular, the so-called dielectric theorem that provides the value of the inverse-energy-weighted sum rule based on the simple knowledge of the ground state is demonstrated. This theorem is applied to the case of constrained calculations of the average excitation energy of the monopole resonance combined with the Thouless theorem. The pairing correlations are shown to have the effect of increasing the polarizability m_{-1} . The detailed analysis of the profile of the strength functions by mean of QRPA reveals that the decrease of the average monopole excitation energies in some isotopes is associated with neutron states that emerge at an energy that is lower than the main giant resonance peak.

DOI: [10.1103/PhysRevC.79.054329](https://doi.org/10.1103/PhysRevC.79.054329)

PACS number(s): 21.60.Jz, 24.30.Cz

I. INTRODUCTION

In physics, one of the most general situations is that concerning a system whose properties can be understood, at least to some extent, by acting on it with an external perturbation. In a formal language, this means that the Hamiltonian \hat{H} that characterizes the system is turned into $\hat{H} + \lambda \hat{Q}$. \hat{Q} is the perturbation and, as usual, a numerical parameter λ is introduced to control its intensity or strength. Perturbation theory can be applied if λ is not too large.

In this article we deal with many-body fermion systems. In particular, we have in mind the atomic nucleus but most of the arguments are rather general. The atomic nucleus can be excited by an external perturbation \hat{Q} (e.g., in nuclear reactions) induced by probes that interact through the strong, electromagnetic, or weak forces. The general problem is that of finding the mean excitation energy associated with a given operator \hat{Q} . In the case of a spherical system, the excited states are identified by the angular momentum and parity quantum numbers, J^π . The operator \hat{Q} is characterized by a given spatial angular momentum L and a given spin S (coupled to total J), as well as by a given isospin T . Linear response theory should be the tool of choice to access the energies E_n and wave functions $|n\rangle$ of the excited states; by means of these quantities, one calculates the excitation probability amplitudes $\langle n|\hat{Q}|0\rangle$, where $|0\rangle$ is the ground state, and the corresponding probabilities. The so-called strength function is defined by

$$S(E) = \sum_n \delta(E - E_n) |\langle n|\hat{Q}|0\rangle|^2, \quad (1)$$

where the transition amplitude $\langle n|\hat{Q}|0\rangle$ can be expressed as the space integral of the transition density $\rho_{ir}^q(\mathbf{r}, n) = \langle n|\sum_i^{N_{orZ}} \delta(\mathbf{r} - \mathbf{r}_i)|0\rangle$ (q denotes neutrons or protons). Then, one can write, respectively,

$$\langle n|\hat{Q}|0\rangle = \int d_3\mathbf{r} Q(\mathbf{r}) [\delta\rho_{ir}^n(\mathbf{r}, n) + \delta\rho_{ir}^p(\mathbf{r}, n)], \quad (2)$$

for an isoscalar operator, and

$$\langle n|\hat{Q}|0\rangle = \int d_3\mathbf{r} \mathbf{Q}(\mathbf{r}) [\delta\rho_{ir}^n(\mathbf{r}, n) - \delta\rho_{ir}^p(\mathbf{r}, n)] \quad (3)$$

for an isovector operator. For nuclear systems, the strength function is often characterized by the appearance of large peaks, absorbing a considerable fraction of the total strength. These peaks are called “giant resonances” [1,2], in keeping also with their line shape that is indeed resonance-like. If we define the moments m_k of the strength function as

$$m_k = \int dE E^k S(E), \quad (4)$$

the mean energy can be defined as the centroid, m_1/m_0 , but this definition can be extended to a whole set of energy ratios

$$\sqrt{\frac{m_k}{m_{k-2}}} \text{ and } \frac{m_k}{m_{k-1}}, \quad (5)$$

which satisfy inequalities like

$$\dots \geq \frac{m_{k+2}}{m_{k+1}} \geq \sqrt{\frac{m_{k+2}}{m_k}} \geq \frac{m_{k+1}}{m_k} \geq \sqrt{\frac{m_{k+1}}{m_{k-1}}} \geq \dots \quad (6)$$

as it can be shown using Schwartz's inequality [3].

Linear response theory means, in the present context, the well-known random-phase approximation (RPA) theory that is described in many textbooks [4,5]. If expressed on a basis, the equations of this theory are written in matrix form and their solutions are found by diagonalization. Nowadays

*Present address: Futura Informatica, via Botticelli 3a, 20020 Villa Cortese (Mi), Italy. luigicapelli@futurainfonline.it

†gianluca.colo@mi.infn.it

‡jun.li@mi.infn.it

RPA diagonalizations are in general quite feasible, although the solution is obviously numerical and the results may not always be fully transparent from a physical point of view. Certainly a progress has been made compared with the time in which the first review articles on sum rules [3,6] were written, because at that time RPA calculations were still much more demanding. However, much of the current activity in nuclear structure theory focuses on the study of exotic nuclei, that is, systems which have different neutron-proton ratios as compared with usual ones. These exotic, neutron-rich or proton-rich, nuclei lie close to the limits of nuclear stability. They are characterized in general by open-shell configurations and the occupied levels lie close to the continuum. For open-shell systems, pairing is known to be important and the independent particle picture is replaced by a quasiparticle one. The linear response theory becomes the quasiparticle RPA (QRPA). In this case, the model space is significantly larger than in the case of RPA. Consequently, QRPA calculations are still demanding nowadays, from the computational point of view: except in the case of low multipoles [7] they often require the use of supercomputers [8]. It should be added that fully self-consistent QRPA calculations that include a proper description of the nuclear continuum are still not available.

In this scenario, *exact* ways to access the sum rule values and the energy centroids are quite relevant for open-shell nuclei. Accordingly, the purpose of the present article is to show *explicitly* the validity of theorems concerning sum rules when pairing is active, that is, within the framework of the HFB plus QRPA theory. To our knowledge, the Thouless theorem has been demonstrated also in the case with pairing, in Ref. [9]. This theorem provides the value of the energy-weighted sum rule (EWSR) m_1 . However, we are not aware of explicit proofs of the so-called dielectric theorem in the case with pairing. This theorem provides the value of the inverse energy-weighted sum rule m_{-1} . We will prove this theorem in the present work. In this way, one can have access to the value of the constrained energy $E_{-1} \equiv \sqrt{\frac{m_1}{m_{-1}}}$ even in systems where pairing is active.

The outline of the article is the following. In Sec. II, we remind the HFB and QRPA theories in the quasiparticle basis shortly. In Sec. III, the dielectric theorem in the framework of HFB plus QRPA is demonstrated. In Sec. IV, this theorem is applied to constrained calculations of the monopole in Ca and Ni isotopes. Finally, there is a short summary in Sec. V.

II. REMINDER OF HFB AND QRPA

Within the independent quasiparticle theory, the nuclear ground state is described by the Hartree-Fock-Bogoliubov (HFB) theory. This theory is based on a linear transformation, namely the general Bogolyubov transformation, which brings the single-particle operators a_l^\dagger, a_l into quasiparticle operators β_k^\dagger, β_k :

$$\beta_k^\dagger = \sum_l U_{lk} a_l^\dagger + V_{lk} a_l \quad (7)$$

$$\beta_k = \sum_l V_{lk}^* a_l^\dagger + U_{lk}^* a_l. \quad (8)$$

On the quasiparticle basis the Hamiltonian of the system, which includes the kinetic energy plus a two-body (possibly density-dependent) interaction,

$$H = \sum_{l_1 l_2} t_{l_1 l_2} a_{l_1}^\dagger a_{l_2} + \frac{1}{4} \sum_{l_1 l_2 l_3 l_4} V_{l_1 l_2 l_3 l_4}^{(\text{as})} a_{l_1}^\dagger a_{l_2}^\dagger a_{l_4} a_{l_3}, \quad (9)$$

can be rewritten as

$$H = H^0 + \sum_{k_1 k_2} H_{k_1 k_2}^{11} \beta_{k_1}^\dagger \beta_{k_2} + \frac{1}{2} \sum_{k_1 k_2} (H_{k_1 k_2}^{20} \beta_{k_1}^\dagger \beta_{k_2}^\dagger + \text{h.c.}) + H_{\text{int}}, \quad (10)$$

where the last term includes all contributions from four quasiparticle operators (in normal ordering). The ground state of this Hamiltonian is the quasiparticle vacuum. This is obtained by setting $H^{20} = 0$; moreover, H^{11} can be put in diagonal form. The corresponding equations are the so-called HFB (or Bogoliubov-De Gennes) equations. Their detailed properties can be found, e.g., in Ref. [4]. Here we only briefly recall that from the solution of the HFB equations one obtains the quasiparticle energies E_k and the wave functions on the (a_l^\dagger, a_l) basis, namely the U and V coefficients. In fact, the HFB equations can be written

$$\begin{pmatrix} h & \Delta \\ -\Delta^* & -h^* \end{pmatrix} \begin{pmatrix} U_k \\ V_k \end{pmatrix} = E_k \begin{pmatrix} U_k \\ V_k \end{pmatrix}, \quad (11)$$

where h and Δ are the mean field and the pairing field whose definition is found in Ref. [4]. The Hamiltonian (10) then becomes

$$H = H^0 + \sum_k E_k \beta_k^\dagger \beta_k + H_{\text{int}}. \quad (12)$$

If one wishes to describe the excited states corresponding to nuclear oscillations, or phonons, one needs to go beyond the static HFB theory. A given vibrational state $|\lambda\rangle$ is produced by the action of a phonon creation operator on the vacuum. This creation operator reads, on a basis made up with two-quasiparticle states,

$$\hat{O}_\lambda^\dagger = \sum_{k_1 > k_2} X_{k_1 k_2}^{(\lambda)} \beta_{k_1}^\dagger \beta_{k_2}^\dagger - Y_{k_1 k_2}^{(\lambda)} \beta_{k_2} \beta_{k_1}. \quad (13)$$

The vacuum $|\tilde{0}\rangle$ is taken as the phonon vacuum, that is, $\hat{O}_\lambda |\tilde{0}\rangle = 0$ for each phonon λ . The time-dependent extension of the HFB equations can be linearized on the given basis of two-quasiparticle states, and a set of equations that provide the energies and the wave functions of a phonon state $|\lambda\rangle$ and that are named QRPA equations, is obtained [4]. These equations are, in explicit form,

$$\begin{pmatrix} A & B \\ -B^* & -A^* \end{pmatrix} \begin{pmatrix} X^{(\lambda)} \\ Y^{(\lambda)} \end{pmatrix} = E_\lambda \begin{pmatrix} X^{(\lambda)} \\ Y^{(\lambda)} \end{pmatrix}. \quad (14)$$

The matrices A and B are given by

$$A_{kk', k'' k'''} = \langle 0 | [\beta_{k'} \beta_k, [\hat{H}, \beta_{k''}^\dagger \beta_{k'''}^\dagger]] | 0 \rangle \quad (15)$$

$$B_{kk', k'' k'''} = -\langle 0 | [\beta_{k'} \beta_k, [\hat{H}, \beta_{k''} \beta_{k'''}]] | 0 \rangle.$$

When the QRPA solutions are known, that is, when the explicit diagonalization of the matrix shown in Eq. (14) is achieved, one can study the transition amplitudes associated with the operator \hat{Q} . In the following, we assume that \hat{Q} is an Hermitian operator and that its expectation value $\langle 0|\hat{Q}|0\rangle$ vanishes; this latter assumption does not imply obviously any loss of generality, because we can always redefine \hat{Q} as $\hat{Q} - \langle 0|\hat{Q}|0\rangle$.

We write the operator \hat{Q} in the quasiparticle basis, namely

$$\hat{Q} = \sum_{ll'} q_{ll'} a_l^\dagger a_{l'} = \sum_{ll'} \sum_{kk'} q_{ll'} [U_{lk}^* U_{l'k'} \beta_k^\dagger \beta_{k'} + U_{lk}^* V_{l'k'}^* \beta_k^\dagger \beta_{k'}^\dagger + V_{lk} U_{l'k'} \beta_k \beta_{k'} + V_{lk} V_{l'k'}^* \beta_k \beta_{k'}^\dagger]. \quad (16)$$

To calculate the matrix elements of \hat{Q} between an excited QRPA state $|\lambda\rangle$ and the ground state $|\tilde{0}\rangle$, we rely on the fact that the derivation of RPA and QRPA is based on the quasiboson approximation. In the case of interest, that is, QRPA, the relevant quasiboson operators are

$$\Gamma_{k_1 k_2}^\dagger \equiv \beta_{k_1}^\dagger \beta_{k_2}^\dagger \quad \Gamma_{k_1 k_2} \equiv \beta_{k_2} \beta_{k_1}. \quad (17)$$

We write

$$\langle \tilde{0}|\hat{Q}|\lambda\rangle = \langle \tilde{0}|[\hat{Q}, \hat{O}_\lambda^\dagger]|\tilde{0}\rangle, \quad (18)$$

in such a way that, after expressing both \hat{Q} and \hat{O}_λ^\dagger in terms of the boson operators (17), the commutator in the last equation is calculated by using the basic boson commutation relations. The result is

$$\langle \tilde{0}|\hat{Q}|\lambda\rangle = \sum_{ll'} \sum_{k>k'} q_{ll'} [X_{kk'}^{(\lambda)} (U_{l'k} V_{lk'} - U_{l'k'} V_{lk}) + Y_{kk'}^{(\lambda)} (U_{lk}^* V_{l'k'}^* - U_{lk'}^* V_{l'k}^*)]. \quad (19)$$

For the sake of convenience, in keeping with what follows and with the results of Refs. [3,9], we prefer to recast this result in the form

$$\langle \tilde{0}|\hat{Q}|\lambda\rangle = (\tilde{q}^\top \tilde{q}^\dagger) \begin{pmatrix} X^{(\lambda)} \\ Y^{(\lambda)} \end{pmatrix}, \quad (20)$$

where \tilde{q} is a vector whose components are the matrix elements $\tilde{q}_{kk'}$, with

$$\tilde{q}_{kk'} = \sum_{ll'} q_{ll'} h_{ll',kk'} \quad (21)$$

and

$$h_{ll',kk'} = U_{l'k} V_{lk'} - U_{l'k'} V_{lk}. \quad (22)$$

III. THEOREMS ON THE MOMENTS OF THE STRENGTH FUNCTION

In a recent work, E. Khan *et al.* [9] have shown the validity of the Thouless theorem for the energy-weighted sum rule (EWSR), in the case of self-consistent QRPA based on HFB. This reads, if $|0\rangle$ is the HFB ground state,

$$\sum_\lambda E_\lambda |\langle \lambda|\hat{Q}|\tilde{0}\rangle|^2 = \frac{1}{2} \langle 0|[\hat{Q}, [\hat{H}, \hat{Q}]]|0\rangle. \quad (23)$$

The aim of this section is to demonstrate the validity of other general theorems concerning the sum rules within the QRPA frame.

In particular, we start by showing what follows.

A. Theorem 1

In the only hypothesis that \hat{Q} is a Hermitian one-body operator, his k -th order moments are given by

$$m_k(\hat{Q})_{\text{QRPA}} = \frac{1}{2} (\tilde{q}^\top \tilde{q}^\dagger) \begin{pmatrix} A & B \\ -B^* & -A^* \end{pmatrix}^k \begin{pmatrix} \tilde{q} \\ -\tilde{q}^* \end{pmatrix}. \quad (24)$$

Let us start from the general expression of the k -th order moment of the operator \hat{Q} [cf. Eqs. (1) and (4)], namely

$$m_k(\hat{Q}) = \sum_{\lambda>0} E_\lambda^k |\langle \lambda|\hat{Q}|\tilde{0}\rangle|^2, \quad (25)$$

where the summation includes only the positive QRPA solutions. The QRPA equations (14) imply that

$$\begin{pmatrix} X^{(\lambda)} \\ Y^{(\lambda)} \end{pmatrix} E_\lambda^k = \begin{pmatrix} A & B \\ -B^* & -A^* \end{pmatrix}^k \begin{pmatrix} X^{(\lambda)} \\ Y^{(\lambda)} \end{pmatrix}. \quad (26)$$

One should remember that if $2N$ is the total number of QRPA solutions, half of them are positive and the other half are negative but equal to the previous ones in absolute value. Consequently, by exploiting this symmetry,

$$\begin{aligned} 2m_k(\hat{Q}) &= 2 \sum_{\lambda=1}^N E_\lambda^k |\langle \lambda|\hat{Q}|\tilde{0}\rangle|^2 = \sum_{\lambda=1}^{2N} |E_\lambda^k| |\langle \lambda|\hat{Q}|\tilde{0}\rangle|^2 \\ &= \left(\sum_{\lambda=1}^N - \sum_{\lambda=N+1}^{2N} \right) (\tilde{q}^\top \tilde{q}^\dagger) \begin{pmatrix} X^{(\lambda)} \\ Y^{(\lambda)} \end{pmatrix} \\ &\quad \times (X^{(\lambda)\dagger} Y^{(\lambda)\dagger}) \begin{pmatrix} \tilde{q} \\ -\tilde{q}^* \end{pmatrix} E_\lambda^k \\ &= \left(\sum_{\lambda=1}^N - \sum_{\lambda=N+1}^{2N} \right) (\tilde{q}^\top \tilde{q}^\dagger) \begin{pmatrix} A & B \\ -B^* & -A^* \end{pmatrix}^k \begin{pmatrix} X^{(\lambda)} \\ Y^{(\lambda)} \end{pmatrix} \\ &\quad \times (X^{(\lambda)\dagger} - Y^{(\lambda)\dagger}) \begin{pmatrix} \tilde{q} \\ -\tilde{q}^* \end{pmatrix}. \quad (27) \end{aligned}$$

If we now insert the closure relation associated with the QRPA solutions [5],

$$\left(\sum_{\lambda=1}^N - \sum_{\lambda=N+1}^{2N} \right) \begin{pmatrix} X^{(\lambda)} \\ Y^{(\lambda)} \end{pmatrix} (X^{(\lambda)\dagger} - Y^{(\lambda)\dagger}) = \begin{pmatrix} 1 & & 0 \\ & \dots & \\ 0 & & 1 \\ & & & 1 \end{pmatrix}, \quad (28)$$

then the thesis follows.

If H is even under time reversal, then A and B can be taken as real, and X and Y are real as well. If \hat{Q} is also even under time reversal its matrix elements are real [10]. Then, it is possible to show with simple algebra that the odd moments of the operator \hat{Q} ($k_{\text{odd}} \equiv 2n + 1$) are given by

$$m_{k_{\text{odd}}}(\text{QRPA}) = \tilde{q}^\top (A - B) [(A + B)(A - B)]^{\frac{k-1}{2}} \tilde{q} \quad (29)$$

and, in particular, we can write

$$m_{-1}(\text{QRPA}) = \tilde{q}^\top (A + B)^{-1} \tilde{q}; \quad (30)$$

for the moment of order -1 . We note, passing by, that the even moments of the operator \hat{Q} ($k_{\text{odd}} \equiv 2n$) are given by

$$m_{k_{\text{even}}}(\text{QRPA}) = \tilde{q}^\top [(A - B)(A + B)]^{\frac{k}{2}} \tilde{q}. \quad (31)$$

We focus our attention on the m_{-1} moment, or ‘‘inverse energy-weighted sum rule’’ (IEWSR). It is known that the IEWSR can be also obtained from constrained Hartree-Fock (CHF) calculations. In particular it has been proven [3] that the results of CHF and the IEWSR from fully self-consistent RPA are directly connected by the dielectric theorem. Our purpose is to demonstrate explicitly that the dielectric theorem is true in the case of QRPA as well. We will focus on the case of QRPA on top of HFB. The simpler case of QRPA on top of HF-BCS can be considered as a special limiting case: in principle it would not need a separate proof, but this is anyway outlined in the Appendix, for the reader’s convenience. The case of RPA on top of HF (already demonstrated) is a further limiting case.

B. Theorem 2 (dielectric theorem in the HFB frame)

Let \hat{Q} be a Hermitian one-body operator. The IEWSR computed in self-consistent QRPA can be obtained also from constrained Hartree-Fock-Bogoliubov (CHFB) calculations, performed with the Hamiltonian $\hat{H} + \lambda \hat{Q}$, as

$$m_{-1}(\text{QRPA}) = -\frac{1}{2} \left[\frac{\partial}{\partial \lambda} \langle \phi(\lambda) | \hat{Q} | \phi(\lambda) \rangle \right]_{\lambda=0} \quad (32)$$

$$m_{-1}(\text{QRPA}) = \frac{1}{2} \left[\frac{\partial^2}{\partial \lambda^2} \langle \phi(\lambda) | \hat{H} | \phi(\lambda) \rangle \right]_{\lambda=0}, \quad (33)$$

where λ is small enough to ensure the validity of perturbation expansions at lowest order and $\phi(\lambda)$ is the solution of CHFB with a given value of λ .

Let us start by analyzing the CHFB solution. This solution $|\phi\rangle$ can be written (aside from a normalization factor) using the Thouless theorem [11] generalized in the HFB case (cf. also Refs. [5,12]),

$$\begin{aligned} |\phi\rangle &= |0\rangle + \frac{1}{1! \times 2!} \sum_{\mu\nu} c_{\mu\nu} \beta_{\mu}^{\dagger} \beta_{\nu}^{\dagger} |0\rangle \\ &+ \frac{1}{2! \times 2^2} \sum_{\mu\nu} \sum_{\mu'\nu'} c_{\mu\nu} c_{\mu'\nu'} \beta_{\mu}^{\dagger} \beta_{\nu}^{\dagger} \beta_{\mu'}^{\dagger} \beta_{\nu'}^{\dagger} |0\rangle \\ &+ \frac{1}{3! \times 2^3} \sum_{\mu\nu} \sum_{\mu'\nu'} \sum_{\mu''\nu''} c_{\mu\nu} c_{\mu'\nu'} c_{\mu''\nu''} \beta_{\mu}^{\dagger} \beta_{\nu}^{\dagger} \beta_{\mu'}^{\dagger} \beta_{\nu'}^{\dagger} \beta_{\mu''}^{\dagger} \beta_{\nu''}^{\dagger} |0\rangle \\ &+ \dots, \end{aligned} \quad (34)$$

where $|0\rangle$ is the HFB ground state and the coefficients c are *a priori* unknown and must be calculated by exploiting the minimum condition

$$\delta(\langle \phi(\lambda) | \hat{H} + \lambda \hat{Q} | \phi(\lambda) \rangle) = 0. \quad (35)$$

The Lagrange multiplier λ is associated with a given expectation value $\delta Q \equiv \langle \phi | \hat{Q} | \phi \rangle$. The notation δQ is consistent

with our previously established condition $\langle 0 | \hat{Q} | 0 \rangle = 0$. We can write, up to second order in the coefficients c ,

$$\begin{aligned} \delta Q &= \frac{1}{2} \sum_{\mu\nu} (\langle 0 | \hat{Q} \beta_{\mu}^{\dagger} \beta_{\nu}^{\dagger} | 0 \rangle c_{\mu\nu} + c_{\mu\nu}^* \langle 0 | \beta_{\nu} \beta_{\mu} \hat{Q} | 0 \rangle) \\ &+ \frac{1}{4} \sum_{\mu\nu} \sum_{\mu'\nu'} c_{\mu\nu}^* \langle 0 | \beta_{\nu} \beta_{\mu} \hat{Q} \beta_{\mu'}^{\dagger} \beta_{\nu'}^{\dagger} | 0 \rangle c_{\mu'\nu'} \\ &+ \frac{1}{8} \sum_{\mu\nu} \sum_{\mu'\nu'} (\langle 0 | \hat{Q} \beta_{\mu}^{\dagger} \beta_{\nu}^{\dagger} \beta_{\mu'}^{\dagger} \beta_{\nu'}^{\dagger} | 0 \rangle c_{\mu\nu} c_{\mu'\nu'} \\ &+ c_{\mu\nu}^* c_{\mu'\nu'}^* \langle 0 | \beta_{\nu'} \beta_{\mu'} \beta_{\nu} \beta_{\mu} \hat{Q} | 0 \rangle) + \dots \end{aligned} \quad (36)$$

By using Eq. (16) one finds that

$$\langle 0 | \hat{Q} \beta_{\mu}^{\dagger} \beta_{\nu}^{\dagger} | 0 \rangle = \sum_{l'l''} q_{ll''} (V_{l\nu} U_{l'\mu} - V_{l\mu} U_{l'\nu}) = \tilde{q}_{\mu\nu} \quad (37)$$

and that

$$\langle 0 | \beta_{\nu} \beta_{\mu} \hat{Q} | 0 \rangle = \sum_{l'l''} q_{ll''} (U_{l\mu}^* V_{l'\nu}^* - U_{l\nu}^* V_{l'\mu}^*) = \tilde{q}_{\mu\nu}^*. \quad (38)$$

The detailed expression of $\langle 0 | \beta_{\nu} \beta_{\mu} \hat{Q} \beta_{\mu'}^{\dagger} \beta_{\nu'}^{\dagger} | 0 \rangle$ can be written but is not needed in what follows; so we simply use for it the shorter notation $\tilde{q}_{\mu\nu, \mu'\nu'}$. We finally use the fact that $\langle 0 | \hat{Q} \beta_{\mu}^{\dagger} \beta_{\nu}^{\dagger} \beta_{\mu'}^{\dagger} \beta_{\nu'}^{\dagger} | 0 \rangle = 0$ and $\langle 0 | \beta_{\nu} \beta_{\mu} \beta_{\nu'} \beta_{\mu'} \hat{Q} | 0 \rangle = 0$. In this way, Eq. (36) can be written

$$\begin{aligned} \delta Q &= \frac{1}{2} \sum_{\mu\nu} (\tilde{q}_{\mu\nu} c_{\mu\nu} + c_{\mu\nu}^* \tilde{q}_{\mu\nu}^*) \\ &+ \frac{1}{4} \sum_{\mu\nu} \sum_{\mu'\nu'} c_{\mu\nu}^* \tilde{q}_{\mu\nu, \mu'\nu'} c_{\mu'\nu'} + \dots \end{aligned} \quad (39)$$

We also need the calculation of the second-order variation δE of the expectation value of the Hamiltonian, that is

$$\begin{aligned} \delta E &= \sum_{\mu\nu} \sum_{\mu'\nu'} \left(\tilde{c}_{\mu\nu}^* A_{\mu\nu, \mu'\nu'} \tilde{c}_{\mu'\nu'} + \frac{1}{2} \tilde{c}_{\mu\nu}^* \tilde{c}_{\mu'\nu'}^* B_{\mu\nu, \mu'\nu'} \right. \\ &\left. + \frac{1}{2} B_{\mu\nu, \mu'\nu'}^* \tilde{c}_{\mu\nu} \tilde{c}_{\mu'\nu'} \right) + \dots \end{aligned} \quad (40)$$

To obtain the previous expression, use has been made of the definitions of the matrices A and B [see Eq. (15)]. Moreover, the notation $\tilde{c}_{\mu\nu} \equiv \frac{1}{2} c_{\mu\nu}$ has been introduced. Finally, if we replace the pair $\mu\nu$ with α , we set $L_{\alpha, \alpha'} \equiv \tilde{q}_{\alpha, \alpha'}$ to avoid confusion, and we consider the matrix elements of \hat{Q} as real (consistently with the previous section), we then arrive at

$$\begin{aligned} \delta E + \lambda \delta Q &= \lambda \sum_{\alpha} (\tilde{q}_{\alpha} \tilde{c}_{\alpha} + \tilde{c}_{\alpha}^* \tilde{q}_{\alpha}) \\ &+ \sum_{\alpha\alpha'} \left(\lambda \tilde{c}_{\alpha}^* L_{\alpha, \alpha'} \tilde{c}_{\alpha'} + \tilde{c}_{\alpha}^* A_{\alpha, \alpha'} \tilde{c}_{\alpha'} \right. \\ &\left. + \frac{1}{2} \tilde{c}_{\alpha}^* \tilde{c}_{\alpha'}^* B_{\alpha, \alpha'} + \frac{1}{2} B_{\alpha, \alpha'} \tilde{c}_{\alpha} \tilde{c}_{\alpha'} \right) + \dots \end{aligned} \quad (41)$$

We wish now to show that the quantity just written, $\delta E + \lambda \delta Q$, has a minimum when

$$\delta Q_{\lambda} = -2\lambda a - 3\lambda^2 b + O(\lambda^3) \quad (42)$$

and

$$\delta E_\lambda = \lambda^2 a + 2\lambda^3 b + O(\lambda^4), \quad (43)$$

with

$$\begin{aligned} a &= \tilde{q}^\top (A + B)^{-1} \tilde{q} \\ b &= -\tilde{q}^\top (A + B)^{-1} L (A + B)^{-1} \tilde{q}. \end{aligned} \quad (44)$$

Because the coefficients \tilde{c} in Eq. (41) are in principle complex, we set $\tilde{c}_\alpha = x_\alpha + iy_\alpha$ and $\tilde{c}_\alpha^* = x_\alpha - iy_\alpha$. After some algebra, Eq. (41) becomes

$$\begin{aligned} \delta E + \lambda \delta Q &= 2\lambda \sum_\alpha x_\alpha \tilde{q}_\alpha + \sum_{\alpha, \alpha'} [x_\alpha (A_{\alpha\alpha'} + B_{\alpha\alpha'}) x_{\alpha'} \\ &\quad + y_\alpha (A_{\alpha\alpha'} - B_{\alpha\alpha'}) y_{\alpha'} \\ &\quad + \lambda (x_\alpha L_{\alpha\alpha'} x_{\alpha'} + y_\alpha L_{\alpha\alpha'} y_{\alpha'})] + \dots, \end{aligned} \quad (45)$$

where use has been made of the fact that the matrices A , B , and L are symmetric. Let us then impose that $E + \lambda Q$ has a minimum, namely

$$\begin{aligned} \frac{\partial(\delta E + \lambda \delta Q)}{\partial x} &= 2\lambda \tilde{q} + 2(A + B + \lambda L)x = 0, \\ \frac{\partial(\delta E + \lambda \delta Q)}{\partial y} &= 2(A - B + \lambda L)y = 0. \end{aligned} \quad (46)$$

We assume that both x and y can be expanded in a power series of λ ,

$$x = \sum_n \lambda^n x^{(n)} \quad y = \sum_n \lambda^n y^{(n)} \quad (47)$$

and we insert these developments in the minimum conditions (46). It is easy to verify that the vector y (i.e., the imaginary part of c) is identically zero at any order in λ . For the real part of c , that is x , we obtain that $x^{(0)} = 0$, that $x^{(1)} = -(A + B)^{-1} \tilde{q}$, and that the recursion relation

$$x^{(n+1)} = -(A + B)^{-1} L x^{(n)} \quad (48)$$

holds $\forall n > 0$. If we derive the explicit expressions of $x^{(n)}$ from Eq. (48) and we insert them into Eq. (45), we arrive at

$$\delta E = \lambda^2 \tilde{q}^\top (A + B)^{-1} \tilde{q} - 2\lambda^3 \tilde{q}^\top (A + B)^{-1} L (A + B)^{-1} \tilde{q} + O(\lambda^4), \quad (49)$$

$$\delta Q = -2\lambda \tilde{q}^\top (A + B)^{-1} \tilde{q} + 3\lambda^2 \tilde{q}^\top (A + B)^{-1} L (A + B)^{-1} \tilde{q} + O(\lambda^3). \quad (50)$$

We write

$$a = \tilde{q}^\top (A + B)^{-1} \tilde{q} \quad (51)$$

and

$$b = -\tilde{q}^\top (A + B)^{-1} L (A + B)^{-1} \tilde{q}, \quad (52)$$

and this completes the proof of Eqs. (42) and (43).

One can, at this point, extract from Eqs. (42) and (43) the result that

$$\begin{aligned} a &= -\frac{1}{2} \left[\frac{\partial}{\partial \lambda} \langle \phi(\lambda) | \hat{Q} | \phi(\lambda) \rangle \right]_{\lambda=0} \\ &= \frac{1}{2} \left[\frac{\partial^2}{\partial \lambda^2} \langle \phi(\lambda) | \hat{H} | \phi(\lambda) \rangle \right]_{\lambda=0}. \end{aligned} \quad (53)$$

Because, a given by Eq. (51), coincides with that of m_{-1} (QRPA) from Eq. (30), this is the proof of the dielectric theorem in the HFB case as it has been stated by means of Eqs. (32) and (33).

IV. APPLICATIONS TO THE ISOSCALAR GIANT MONOPOLE RESONANCE

In the case of the isoscalar giant monopole resonance (ISGMR), the operator \hat{Q} has the form

$$\hat{Q} = \sum_{i=1}^A r_i^2. \quad (54)$$

Then the EWSR and IEWSR are given, respectively, by

$$m_1(\hat{Q}) = \frac{2\hbar^2}{m} A \langle r^2 \rangle_{\text{HFB}} \quad (55)$$

and

$$m_{-1}(\hat{Q}) = -\frac{1}{2} \left[\frac{\partial}{\partial \lambda} \langle r^2 \rangle_{\text{HFB}} \right]_{\lambda=0} = \frac{1}{2} \left[\frac{\partial^2}{\partial \lambda^2} \langle H \rangle_{\text{HFB}} \right]_{\lambda=0} \quad (56)$$

In the present numerical study, both the unconstrained and constrained solutions of the HFB equations are obtained in the coordinate representation by using a spherical box. We also need a cutoff on the quasiparticle energy and this value is set at 60 MeV; the value of the box radius is discussed below. In the particle-hole channel, we use the SKM* Skyrme force [13]. In the particle-particle channel, we use for simplicity the zero-range volume pairing force that has the simple form

$$v_{\text{pair}} = V_0 \delta(\mathbf{r}_1 - \mathbf{r}_2). \quad (57)$$

In our calculations, the value of the parameter V_0 is fixed at -183.9 MeV fm^3 by fitting the experimental data of the mean neutron gap in ^{44}Ca ($\Delta = 1.49 \text{ MeV}$).

The self-consistency of the QRPA calculations requires the use in QRPA of a residual force derived from the HFB fields. In the spherical QRPA solution, there exists the problem of a spurious state in the monopole channel due to the particle number symmetry broken by the HFB solution [4]. The spurious state has a contribution to the moments of the strength function, and it must be projected out from the real physical states [7].

The accuracies of both the CHFB and the HFB-QRPA calculations have been carefully tested in the case of the Ca isotopes. There is no special difficulty in performing CHFB and the results from this approach seem quite reliable. However, as already pointed out in our previous work [7], QRPA calculations are rather demanding when performed using the canonical basis. In most of the cases the agreement between m_{-1} from CHFB and QRPA is at the level of a few percentages, which is deemed to be satisfactory. For instance, in the case of ^{42}Ca , the value of the m_{-1} from CHFB is $m_{-1} = 95.98 \text{ MeV}^{-1} \text{ fm}^4$ (this is obtained from the first derivative of $\langle r^2 \rangle_{\text{HFB}}$, whereas from the second derivative of $\langle H \rangle_{\text{HFB}}$ one finds $95.68 \text{ MeV}^{-1} \text{ fm}^4$; in the following discussion we will as a rule present the values obtained from the first derivative of $\langle r^2 \rangle_{\text{HFB}}$ only). Using

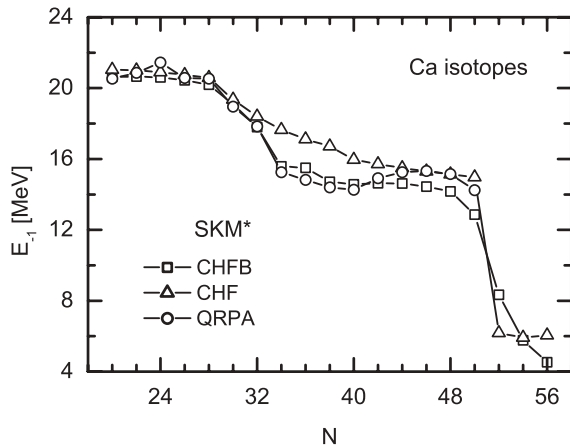


FIG. 1. Constrained monopole energies in the Ca isotope chain obtained with the SKM* force. In the CHF B and QRPA calculations, a volume pairing force is used. See the text for a detailed discussion.

the value of m_1 from the double commutator, one obtains $E_{-1} = 20.66$ MeV. The QRPA exhausts almost all the EWSR (99.93%), and it gives as results $m_{-1} = 93.99$ MeV $^{-1}$ fm 4 , and $E_{-1} = 20.87$ MeV. There are, however, a few cases where QRPA results differ more than 5–6% from the CHF B ones. This happens when pairing is strong or for large neutron numbers. In this latter case, we must use a large box (neutrons are weakly bound) so that very accurate QRPA calculations become almost prohibitive in keeping with the size of the basis.

As an additional test, we have verified that in the case without pairing, for example in ^{40}Ca , the CHF calculation produces values for the IEWSR and the constrained energy, $m_{-1} = 90.0$ MeV $^{-1}$ fm 4 and $E_{-1} = 20.65$ MeV, respectively, that are in good agreement with Ref. [14]; the results from the RPA calculation are $m_{-1} = 88.76$ MeV $^{-1}$ fm 4 , $E_{-1} = 20.53$ MeV.

In Fig. 1, we display the constrained monopole energies for the Ca isotopes as a function of the neutron number. From ^{40}Ca to ^{70}Ca , the radius of the box used in the constrained calculations is 12.5 fm (with a mesh of 0.1 fm), whereas from ^{72}Ca to ^{76}Ca a large box radius (40 fm) is needed for convergence of the CHF and CHF B calculations. As we discuss below, the drop of m_{-1} beyond ^{70}Ca is not due to the change in the procedure but to physical reasons (the polarizability increases as weakly bound neutron orbitals are filled). We could, in principle, have performed all calculations with a box of 40 fm. Indeed, in the case e.g. of ^{68}Ca we obtain values of m_{-1} from CHF B, using either the large box of 40 fm or the small box of 12.5 fm, which are equal to 471.98 and 467.67 MeV $^{-1}$ fm 4 , respectively.

Along the Ca isotopic chain the constrained excitation energies decrease always when the number of neutrons evolves from the stable nuclei toward the neutron drip line. There are five distinct regions along the chain as far as the comparison of the results of CHF B and CHF calculations is concerned. In the region from ^{40}Ca to ^{48}Ca , the excitation energies decrease rather smoothly when increasing the number of neutrons, because with pairing more states are occupied and give rise

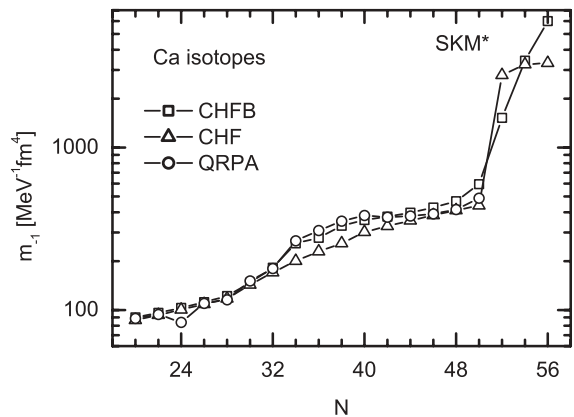


FIG. 2. Same as described in the caption to Fig. 1 but for the monopole IEWSR.

to low-energy excitations (or, in other words, increase the polarizability of the system). In the region from ^{48}Ca to ^{52}Ca , although the pairing correlations are not strong, the occupation of the $2p_{3/2}$ orbit has a great contribution to decrease the excitation energies. In the region from ^{52}Ca to ^{60}Ca , there is a difference between the CHF and the CHF B calculations. In the CHF calculation, the orbit $2p_{1/2}$ is empty while it is partially occupied when including the effect of pairing. This low l orbit gives a definite contribution to the polarizability of the system, and decreases the excitation energies markedly. In the region from ^{60}Ca to ^{70}Ca , the $2p_{1/2}$ orbit is fully occupied in the CHF calculation. Therefore there is small difference between the CHF and CHF B calculations. From ^{70}Ca to the neutron drip-line nuclei (^{76}Ca), there is a strong decrease of the excitation energies in the CHF and CHF B calculations. This great reduction is due to the even longer tails of $3s_{1/2}$ and $2d_{5/2}$ orbits.

We have analyzed whether the changes in the constrained monopole energies come mainly from changes in the values of m_1 or m_{-1} . From Eq. (55), one can observe that the EWSR is sensitive to the value of the mean square radius. As HFB and HF calculations give almost the same mean square radii, the differences in the constrained monopole energies come from the IEWSR. Figure 2 gives constrained estimates of the IEWSR for the Ca isotopes as a function of the neutron number: the IEWSR shows a similar global tendency as the excitation energies.

In the stable region along the calcium isotopes, we have checked that the constrained HF-BCS calculations give very similar values of the IEWSR as CHF B, while in the very neutron-rich region this is not the case. For example, in ^{44}Ca , the IEWSR from the CHF B and constrained BCS are 103.1 and 105.5 MeV $^{-1}$ fm 4 , while in ^{66}Ca , they are 402.6 and 466.9 MeV $^{-1}$ fm 4 , respectively. The difference is mainly attributed, in this case, to the long tails of some orbits like $1f_{5/2}$ that increases the polarizability m_{-1} in the case of constrained HF-BCS. The CHF B calculation reduces this tail, due to the self-consistency between the pairing channel and the mean field. We believe this is an example that shows that constrained HF-BCS is inappropriate for the very neutron-rich nuclei.

If there is a change in E_{-1} , as it is for Ca isotopes above ^{70}Ca , using the CHF B calculations we are not able to tell if this

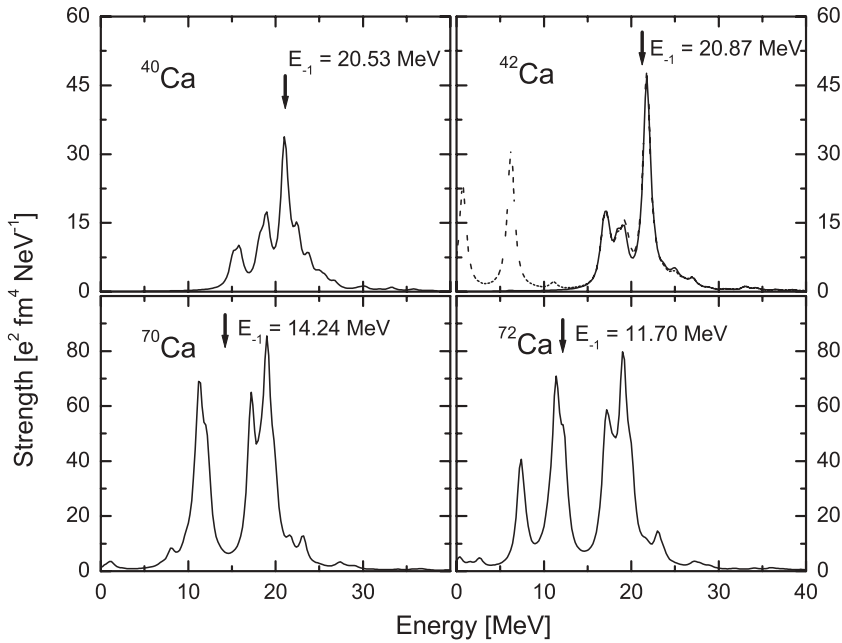


FIG. 3. Isoscalar 0^+ strength functions for ^{40}Ca , ^{42}Ca , ^{70}Ca , and ^{72}Ca with the SKM* force and the volume pairing force. The dashed line in the panel of ^{42}Ca is the result including the contribution of the spurious state.

is due to a decrease of E_{ISGMR} or to the appearance of new, low-lying modes. Therefore, we have made detailed QRPA calculations for $^{70,72}\text{Ca}$ (despite the previous warnings, these can be nonetheless illustrative). Figure 3 shows the isoscalar 0^+ strength functions for ^{40}Ca , ^{42}Ca , ^{70}Ca , and ^{72}Ca with the SKM* force and the volume pairing force. There exists a usual giant monopole mode around 19 MeV and a low-lying mode around 12 MeV with similar strengths in ^{70}Ca and ^{72}Ca . But in ^{72}Ca , there is another less collective peak at lower energy. This new low-lying mode gives to the average excitation energies the great drop that has been seen in Fig. 1. Figure 4 displays the

proton and neutron transition densities in $^{70,72}\text{Ca}$ in the peaks of the strength function that are visible in Fig. 3. Protons have little contribution to the low-lying modes. Thus these low-lying modes are kind of neutron modes, and they show structures in the inner part of the nucleus with a peak at the surface. The usual giant monopole mode has a rather clear isoscalar character.

The spurious state gives a contribution to the moments of the strength function if it is not carefully projected out. This is quite clear if one looks at the panel of Fig. 3 that refers to ^{42}Ca . As the spurious strength function appears only

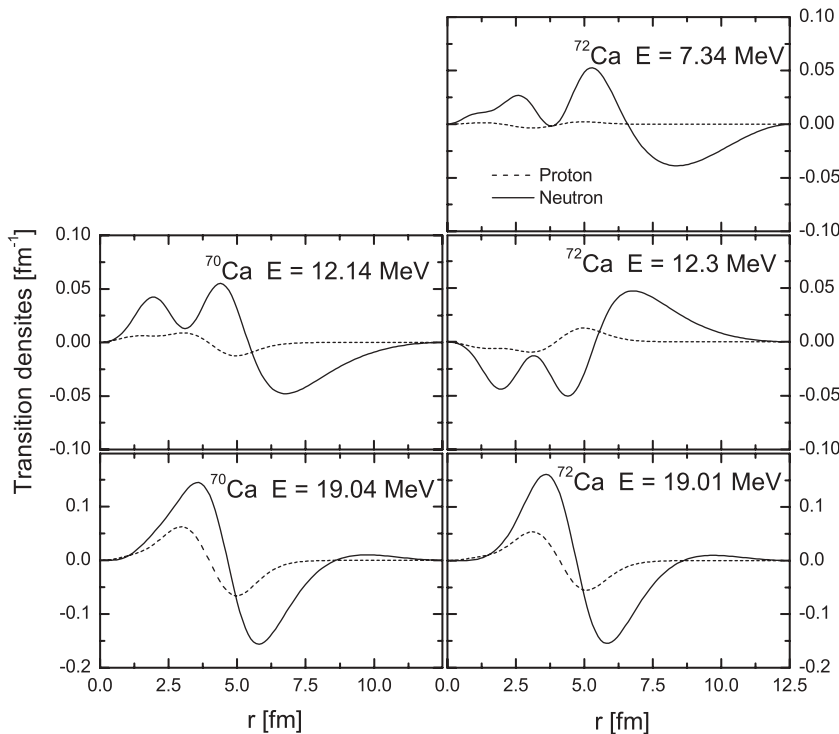


FIG. 4. Proton and neutron transition densities in $^{70,72}\text{Ca}$ in the peaks of the strength function in Fig. 3.

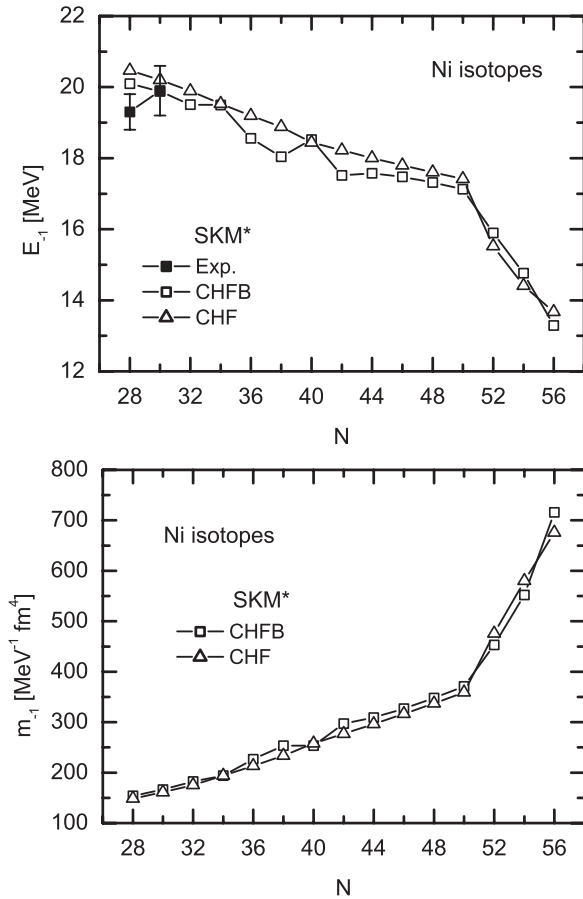


FIG. 5. Excitation energies (upper) and the inverse energy-weighted sum rule (lower) of the isoscalar giant monopole resonance in the nickel isotopes with SKM* force. In CHFb calculations, the pairing force used is volume pairing. The experimental data are extracted from Refs. [15,16].

at low energy, its error on the EWSR is negligible, but that on the IEWSR could be very large. For example, in the case of ^{42}Ca , if one projects out the spurious strength completely, the values of the EWSR, IEWSR, and the monopole constrained energy are $m_1 = 4.1 \times 10^4 \text{ MeV fm}^4$, $m_{-1} = 93.99 \text{ MeV}^{-1} \text{ fm}^4$, and $E_{-1} = 20.87 \text{ MeV}$, while they are $m_1 = 4.75 \times 10^4 \text{ MeV fm}^4$, $m_{-1} = 821.11 \text{ MeV}^{-1} \text{ fm}^4$, and $E_{-1} = 7.61 \text{ MeV}$ when including the contribution of the spurious strength.

Figure 5 shows the constrained monopole energies (upper panel), as well as the inverse energy-weighted sum rule value (lower panel) for the Ni isotopes. Numerically, in the region from ^{56}Ni to ^{78}Ni , the radius of the box is fixed at 15 fm and this ensures the convergence of the calculations, while in the region from ^{80}Ni to ^{84}Ni , the box radius is extended to 25 fm for convergence. In the constrained HFB calculations, we use the same quasiparticle energy cutoff and same Skyrme and pairing forces as already discussed for the Ca isotopes. In general, the constrained HF and HFB calculations give roughly similar excitation energies and inverse energy-weighted sum rules along the considered chain from ^{56}Ni to the neutron drip line. From ^{56}Ni to ^{78}Ni ,

the excitation energies decrease slowly when the number of neutrons increases. The differences between the CHF and CHFb results in ^{64}Ni and ^{66}Ni come from the contribution of the neutron $2p_{1/2}$ orbit that is partly occupied when including the pairing effect, while the differences from ^{70}Ni to ^{76}Ni are due to the contribution of the neutron $2d_{5/2}$ orbit. From ^{78}Ni to the neutron drip line, the excitation energies decrease steeply because there exists an important contribution of the neutron $2d_{5/2}$ orbit both in constrained HF and HFB calculations. It is worth analyzing the decrease of the energy above ^{78}Ni also by means of QRPA. Figure 6 shows the isoscalar 0^+ strength functions for $^{58,76,78,80,82,84}\text{Ni}$. The decrease of the constrained energy is associated with the gradual development of peaks below the main giant resonance peak. These low-lying modes are expected to be associated with the neutron excess, similarly to what already discussed for Ca isotopes. Figure 7 presents the proton and neutron transition densities in $^{76,78,80,82,84}\text{Ni}$ in the peaks of the strength function in Fig. 6. When the number of neutrons increases, protons decrease their contributions to the low-lying modes ($E \leq 15 \text{ MeV}$), and they have structures in the interior and a peak at the surface of the nuclei. In $^{82,84}\text{Ni}$, these low-lying modes are kinds of neutron modes.

V. SUMMARY

In this article, we have demonstrated the validity of the dielectric theorem in the framework of HFB plus QRPA. This theorem has been used to calculate the polarizability m_{-1} in the case of monopole, along the Ca and Ni isotopes. Together with the value of m_1 obtained with the Thouless theorem, this provides an estimate of the average monopole excitation energy. Our method for extracting the polarizability is in good agreement with QRPA.

For a Skyrme force like SkM* and a volume pairing force, along the Ca isotopes, the global trend of the average monopole energies is associated with a continuous decrease as the number of neutrons increases. The pairing correlations have an attractive effect that increases the polarizability m_{-1} compared with the CHF calculations of Ref. [14]. This behavior of the polarizability reveals that the orbits close to the Fermi surface affect the IEWSR and the average monopole excitation energies.

There exists a great drop above ^{70}Ca of the average monopole excitation energy. The detailed analysis of the profile of the strength functions by means of HFB-QRPA, performed in the mass region where there is a great decrease of the average monopole excitation energy, reveals that this decrease comes from peaks at lower energy than the ISGMR. The transition densities calculated at these peaks show that these low-lying modes are kinds of neutron modes. Similar CHFb calculations in the Ni isotopes show that the decrease of the average monopole excitation energies is associated with a more gradual development of peaks lying below the main giant resonance peak. The constrained HF-BCS calculations give similar values of the IEWSR as CHFb in the stable nuclei, while they seem to be (as it can be expected) inappropriate for the very neutron-rich nuclei.

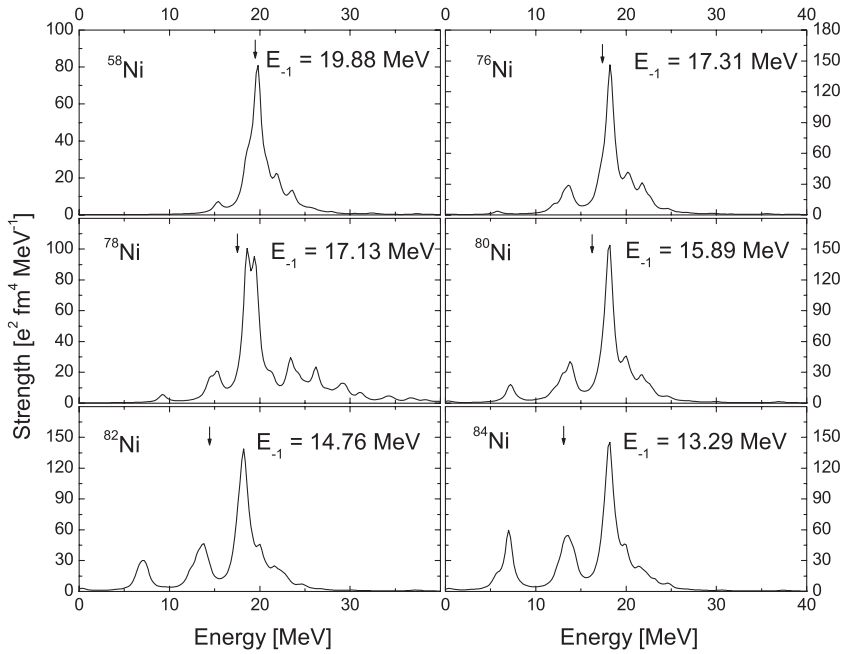


FIG. 6. Same as described in the caption to Fig. 3 but for the Ni isotopes.

Having shown the validity of the dielectric theorem paves the way to further applications. The theorem could be used to test other QRPA frameworks (e.g., those including the continuum) and/or to test implementations based on more general functionals than those based on the usual Skyrme force plus the zero-range, density-dependent pairing. Operators other than the monopole one can be used if one has a deformed code at his disposal. We believe that constrained estimates of the average excitation energies are useful to have a quick idea of the general trends along isotopic, or isotonic, chains.

Of course they cannot replace full QRPA calculations, which are, however, very time-consuming and should be performed in those cases where they are expected to elucidate real novel features of the excitation spectra.

APPENDIX: THE DIELECTRIC THEOREM IN THE HF-BCS FRAME

The HF plus BCS (Bardeen-Cooper-Schrieffer) case can be considered as a special limit of the HFB theory in which the

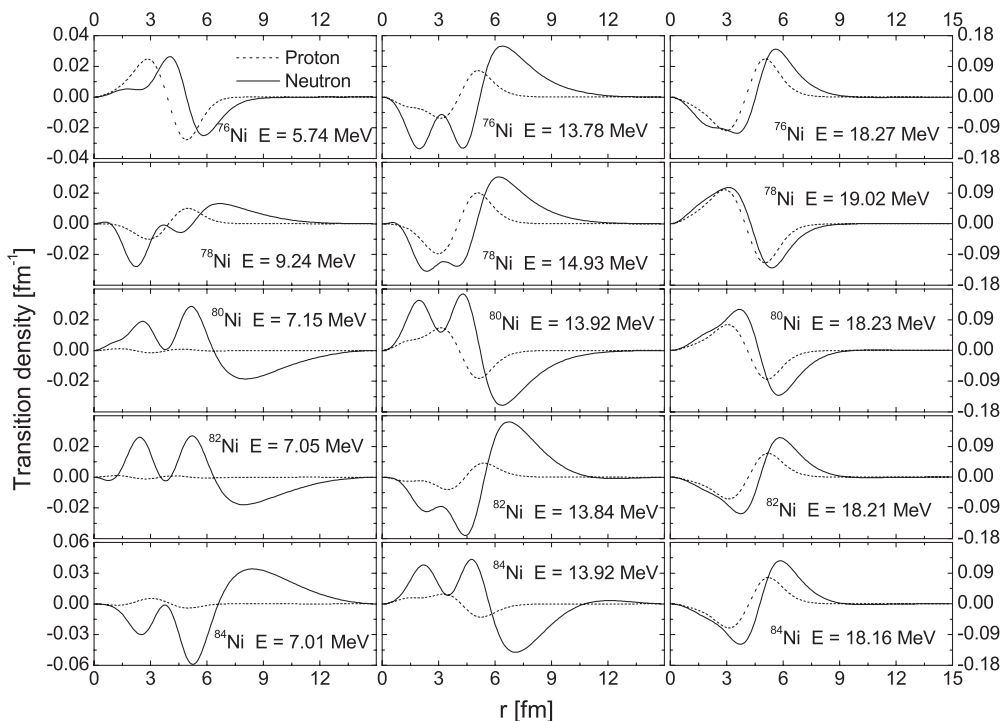


FIG. 7. Same as described in the caption to Fig. 4 but for the Ni isotopes.

pairing field Δ [cf. Eq. (11)] is diagonal in the basis of the eigenstates of the mean field h . As a consequence, the general Bogolyubov transformation reduces to

$$\beta_k^\dagger = u_k a_k^\dagger - v_k a_{\bar{k}} \quad (\text{A1})$$

$$\beta_k = u_k a_k - v_k a_{\bar{k}}^\dagger, \quad (\text{A2})$$

where the bar labels a time-reversal state [4]. The inverse transformations are

$$a_k^\dagger = u_k \beta_k^\dagger + v_k \beta_{\bar{k}} \quad (\text{A3})$$

$$a_k = u_k \beta_k + v_k \beta_{\bar{k}}^\dagger. \quad (\text{A4})$$

It is not strictly necessary to repeat step by step the proof of the dielectric theorem in this special case. Equation (34) holds in the HF plus BCS case as well. The operator can be written

$$\begin{aligned} \hat{Q} = \sum_{kk'} q_{kk'} a_k^\dagger a_{k'} = \sum_{kk'} q_{kk'} [u_k u_{k'} \beta_k^\dagger \beta_{k'}^\dagger + u_k v_{k'} \beta_k^\dagger \beta_{\bar{k}'}^\dagger \\ + v_k u_{k'} \beta_{\bar{k}} \beta_{k'} + v_k v_{k'} \beta_{\bar{k}} \beta_{\bar{k}'}^\dagger], \end{aligned} \quad (\text{A5})$$

and this corresponds to Eq. (16) with the simple replacements $U_{lk} = u_k \delta(lk)$ and $V_{lk} = v_k \delta(l\bar{k})$. With the same replacements Eq. (19) becomes

$$\begin{aligned} \langle \tilde{0} | \hat{Q} | \lambda \rangle = \sum_{k>k'} q_{\bar{k}k'} X_{kk'}^{(\lambda)} (u_k v_{k'} - \tau u_{k'} v_k) \\ + q_{k\bar{k}'} Y_{kk'}^{(\lambda)} (u_k v_{k'} - \tau u_{k'} v_k), \end{aligned}$$

where τ is +1 if the operator is even under time reversal. From this formula, one deduces that Eq. (20) is valid with the definition (21) replaced by

$$\tilde{q}_{kk'} = q_{k\bar{k}'} (u_k v_{k'} - u_{k'} v_k). \quad (\text{A6})$$

The proof of the dielectric theorem is exactly the same of the main text, with this simpler definition of \tilde{q} : in fact, with it the equality between the first and last members of Eqs. (37) and (38) is still valid. The detailed expression of $\tilde{q}_{\mu\nu, \mu'\nu'}$ has been said to be not needed. Consequently, the reader can follow the steps from Eq. (39) to the end of Sec. III and obtain the proof of the theorem also in the HF plus BCS framework.

-
- [1] P. F. Bortignon, A. Bracco, and R. A. Broglia, *Giant Resonances: Nuclear Structure at Finite Temperature* (Harwood Academic, New York, 1998).
- [2] M. N. Harakeh and A. M. Van Der Woude, *Giant Resonances: Fundamental High-Frequency Modes of Nuclear Excitation* (Oxford University Press, Oxford, 2001).
- [3] O. Bohigas, A. M. Lane, and J. Martorell, Phys. Rep. **51**, 267 (1979).
- [4] P. Ring and P. Schuck, *The Nuclear Many-Body Problem* (Springer-Verlag, New York, 1980).
- [5] D. J. Rowe, *Nuclear Collective Motion* (Methuen and Co. Ltd., London, 1970).
- [6] E. Lipparini and E. S. Stringari, Phys. Rep. **175**, 103 (1989).
- [7] J. Li, G. Colò, and J. Meng, Phys. Rev. C **78**, 064304 (2008).
- [8] J. Terasaki, J. Engel, M. Bender, J. Dobaczewski, W. Nazarewicz, and M. Stoitsov, Phys. Rev. C **71**, 034310 (2005); J. Terasaki and J. Engel, Phys. Rev. C **74**, 044301 (2006).
- [9] E. Khan, N. Sandulescu, M. Grasso, and N. V. Giai, Phys. Rev. C **66**, 024309 (2002).
- [10] K. Goeke, A. M. Lane and J. Martorell, Nucl. Phys. **A296**, 109 (1978).
- [11] D. J. Thouless, Nucl. Phys. **21**, 225 (1960).
- [12] M. Waroquier, J. Ryckebusch, J. Moreau, K. Heyde, N. Blasi, S. Y. van der Werf, and G. Wenes, Phys. Rep. **148**, 249 (1987).
- [13] J. Bartel, P. Quentin, M. Brack, C. Guet, and H.-B. Håkansson, Nucl. Phys. **A386**, 79 (1982).
- [14] M. Centelles, X. Vinas, S. K. Patra, J. N. De, and T. Sil, Phys. Rev. C **72**, 014304 (2005).
- [15] C. Monrozeau, E. Khan, Y. Blumenfeld *et al.*, Phys. Rev. Lett. **100**, 042501 (2008).
- [16] B. K. Nayak *et al.*, Phys. Lett. **B637**, 43 (2006).